frontiers | Frontiers in Materials

TYPE Original Research
PUBLISHED 05 September 2022
DOI 10.3389/fmats.2022.962279

OPEN ACCESS

EDITED BY
Yuli Wang,
Henan Polytechnic University, China

REVIEWED BY
Guo Wen Sun,
Shijiazhuang Tiedao University, China
Yingli Gao,
Changsha University of Science and Technology, China
Zhiyong Liu,
Southeast University, China

*CORRESPONDENCE
Zaibo Li,
lzb381598@163.com

SPECIALTY SECTION
This article was submitted to Structural Materials,
a section of the journal
Frontiers in Materials

RECEIVED 06 June 2022
ACCEPTED 25 July 2022
PUBLISHED 05 September 2022

CITATION
He T, Xu Z, Li Z, Zhao X, Zhao S and Liu Y (2022), Study on the relationship between the particle size distribution characteristics of ground granulated blast furnace slag and its mortar properties.
Front. Mater. 9:962279.
doi: 10.3389/fmats.2022.962279

Study on the relationship between the particle size distribution characteristics of ground granulated blast furnace slag and its mortar properties

Tusheng He, Zengwei Xu, Zaibo Li*, Xuguang Zhao, Sanyin Zhao and Yang Liu

School of Chemistry and Civil Engineering, Shaoguan University, Shaoguan, China

This study adopted the Rosin-Rammler-Bennett (RRB) equation to model the particle size distribution (PSD) of ground granulated blast furnace slag (GGBFS) and prepared four groups of GGBFS powders with a characteristic particle size D_e = 8–20 μm and uniformity coefficient n = 0.9–1.4 by means of grading and combining blast furnace slag. In cases both with and without polycarboxylate superplasticizers (PCE), the fluidity and strength of the mortar were measured. The study found that without PCE, the aggregation of GGBFS had a significant negative impact on the mortar fluidity and hardened paste strength. With the addition of PCE, the properties of the mortar mainly depended on two factors, the specific surface area of the GGBFS and the differences in D_e and n between the GGBFS and Portland cement. At a given specific surface area of GGBFS, high hardened paste strength can be obtained through simultaneously lowering the D_e and increasing the n.

KEYWORDS

ground granulated blast furnace slag, particle size distribution, mortar properties, characteristic particle size, uniformity coefficient

Introduction

Reducing the consumption of natural resources and enhancing the performance of cement and concrete are the two most important issues in the development of cement and concrete in the world today (Akca and Zihnioğlu, 2013; Evi, 2017). A powerful approach to address these problems is the widespread use of industrial waste with potential hydraulic activity, such as blast furnace slag, fly ash, steel slag, and silica fume, to prepare concrete admixtures (Abu-Eishah et al., 2012; Juenger and Siddique, 2015; Yu et al., 2015). Ground granulated blast furnace slag (GGBFS) used as a concrete admixture possesses advantages including excellent mechanical properties, small slump loss over time, and low hydration heat, dependent on the microaggregate effect to a large extent (Teng et al., 2013; Kovtun et al., 2015; Zhang and Li, 2016; Luo et al., 2019).

In the actual industrial production process of GGBFS, the fineness of the powder is controlled by various indexes, for example, sieve residue characterized by a specific pore diameter, specific surface area, and particle size distribution (PSD). Nevertheless, with the same sieve residue or specific surface area, GGBFS powders of different particle size distributions can be obtained, and their properties can vary. Therefore, the PSD is a fineness parameter with a clear quantitative relation to the properties of GGBFS, and regulating this parameter is the ultimate goal of powder fineness control (Binici et al., 2007; Liu et al., 2020). Studies have been published on the influences of the PSD of GGBFS on activity indexes and concrete properties.

Many researchers have performed a large amount of work and proposed various PSD models (Sprung et al., 1985; Tsivilis and Parissakis, 1995; Zhao et al., 2017; Gao et al., 2018). Horsfield (Horsfield, 1932) put forward the closest packing model of powder based on the closest packing theory of rigid spheres. It is assumed that the primary particles are the most closely packed hexagonal particles, and the hexahedral and tetrahedral pores are filled with secondary and tertiary particles respectively. The fourth and fifth time particles are respectively filled in the pores between the primary particles and the second and third time particles, and the remaining pores are finally filled by very small equal diameter particles, which can achieve the minimum porosity of 3.9%. However, the Horsfield model is only applied to ideal non-continuous particle systems, in which all physical and chemical forces are neglected.

Fuller distribution is a classical wide PSD and was originally applied to concrete aggregates. It can also be applied to inert or low hydraulic activity powders after modification by Kuhlmanm (Kuhlmanm et al., 1985). The purpose of Fuller distribution is to achieve maximum packing density regardless of undesirable workability or fluidity caused by rapid hydration of fine cement clinker particles. Thus, cements with Fuller distribution are characterized by their high water requirement and high early strength, while the late strengths of these cements are relatively low due to high water requirement and large amounts of unhydrated cement particles (more than 40% by mass). The Fuller distribution can lead to ideal GGBFS powder stacking results (Celik, 2009; Ye et al., 2017; Xiao et al., 2018). However, in large-scale industrial production, the use of multistage separation and combination to formulate GGBFS powders is not practical (Isaia et al., 2003).

The PSD model proposed by Tsivilis mainly considered the influence of the PSD on the hydration of Portland cement and aimed to improve the later-stage strength of cement concrete (Tsivilis et al., 1990; Çetin et al., 2016). The research object of Tsivilis distribution is Portland cement. The 80 μm sieve residue of Portland cement conforming to Tsivilis distribution is small [R (80) = 0.9%], but the specific surface area is small (s = 352 m^2/kg), and the particle distribution is narrow (concentrated in 3–30 μm). The cement conforming to Tsivilis distribution has low water demand for standard consistency, high porosity of slurry, low hydration heat release, low early strength, but high late strength.

Extensive research and production efforts have demonstrated that the Rosin-Rammler-Bennett (RRB) distribution is the most widely used particle grade model in the field of cement production (Wang et al., 1999). Although there could be minor deviations in the fine particle content when using the RRB equation as the PSD model of GGBFS to describe ultrafine mechanically ground powder, the results generally match the actual distribution of GGBFS. Additionally, the expression of this equation is relatively simple (Kashani et al., 2014; Camalan, 2019).

This study adopted the RRB equation to model the PSD of GGBFS and prepared multiple GGBFS powders with different characteristic particle size D_e and uniformity coefficient n values by means of grading and combining. In cases both with and without polycarboxylate superplasticizers (PCE), the fluidity and strength of the mortar were tested. D_e and n were used as the characteristic indexes of the PSD of GGBFS to reveal the internal relationships between the PSD characteristics and the fluidity and strength of the mortar. The research results elucidate the GGBFS activity effect and microaggregate effect. More importantly, the PSD of GGBFS can be optimized through proper techniques and processes, and the application quality of GGBFS powder can be improved without needing to raise the powder production cost, which has practical significance.

Materials and methods

Materials

This study used 42.5 P.II Portland cement with a Blaine specific surface area of 381 m^2/kg. Granulated blast furnace slag was provided by Baowu Group Guangdong Shaoguan Steel Co., Ltd. Table 1 lists the chemical composition and density of raw materials.

GGBFS powder preparation method

The GGBFS were ground using a lab vertical mill (TRM 3.6). By adjusting the grinding parameters, GGBFS with different PSD characteristics were obtained, which were used as the basic materials for preparing the test GGBFS powders. In order to quantitatively describe and compare the PSDs, the Rosin-Rammler-Bennett (RRB) equation is used.

$$R_D = 100 \cdot e^{-\left(D/De\right)^n} \quad (1)$$

Here, R_D (%) is the cumulative percentage of particles with diameter greater than D (μm). The parameter D_e (μm) is the characteristic particle size, corresponding to the particle size

TABLE 1 Density and chemical compositions of GGBFS and cement (wt%).

Materials	CaO	SiO_2	Al_2O_3	Fe_2O_3	MgO	LOI	Density (g/cm^3)
Cement	63.38	20.82	5.83	3.43	2.65	2.45	3.17
GGBFS	34.24	31.14	19.33	1.03	11.75	0.01	2.92

with an oversize percentage of $100e^{-1}$ (i.e. 36.8%), and the uniformity coefficient n describes the width of the distribution, with a wider distribution corresponding to smaller n, and vice versa.

Twenty-two test GGBFS powders in four groups meeting the research requirements were formulated by grading and combining the basic materials. The formulation targets were as follows: the PSD of all GGBFS powders conformed to the RRB equation, the D_e values of the GGBFS were 8 μm, 12 μm, 16 μm and 20 μm, and n was within the range 0.90–1.40.

A laser particle size analyzer (Malvern Mastersizer 2000) was used to analyze the composition of the test GGBFS powders.

Two groups of mortar pastes were prepared with and without the addition of 0.6% PCE. During the mortar molding process, the water-cement ratio was 0.5:1 when PCE was not added, and the water-cement ratio was 0.37:1 when 0.6% PCE was added.

Fluidity and strength measurement

Cement mortar prisms measuring 40 mm × 40 mm × 160 mm are prepared for fluidity and strength measurements according to ISO 679: 2009 Cement—Test methods—Determination of strength and Chinese National Standard GB/T 18,046–2017 Ground granulated blast furnace slag used for cement and concrete.

Chemically bound water

Portland cement and GGBFS were mixed in a 1:1 ratio. Water was added to reach a water/cement ratio (W/C) of 0.36. After stirring, the cement paste was sealed in plastic bags and cured under standard curing conditions for 3, 7, and 28 days, and the hydration was then stopped using absolute ethanol. The chemically bound water was calculated through measuring the high-temperature ignition loss of the pastes at 950°C.

Interfacial structure

The interfacial structure of hardened cement pastes blended with GGBFS was analyzed using a ZEISS EVO 18 Research scanning electron microscope (SEM) equipped with an energy dispersive spectrometer (EDS).

Results

Preparation of test GGBFS powders

According to the GGBFS powder preparation method described above, 22 test GGBFS powders in four groups were obtained that met the requirements of this study. The specific surface area, D_e, and n of the prepared test GGBFS powders are shown in Table 2. To facilitate analysis of the results, the relationships between the specific surface area and the D_e and n of each test GGBFS powder are depicted in the contour map shown in Figure 1. The particle size distribution is present in Figure 2.

Particle morphology of GGBFS

Figure 3 displays the particle morphologies of GGBFS at each particle grade. The common feature is that the coarse particles larger than 10 μm are mostly gravel-like. The particles have a regular shape, very dense structure, and smooth cross-sections. A few particles have abrasion traces at their edges. Moreover, at the cross-sections and edges of certain particles, there exist round pits caused by the shrinkage induced by the rapid cooling inside of particles during particle breakage, whose diameters range from several micrometers to dozens of micrometers. In the slag powders, most of the particles with a grade lower than 5 μm have a typical broken glass appearance. Their cross-sections are cambered and smooth, but the edges and corners are very sharp and have irregular shapes. There are no abrasion marks at the edges.

Mortar fluidity and strength of GGBFS without PCE

The influence of the PSD characteristics (D_e and n values) of each test GGBFS on mortar fluidity and activity indexes without the addition of PCE, as well as their trends, are shown in Figures 2–4.

Comparing Figures 1, 4 shows that when the specific surface area of GGBFS without PCE was approximately 400 m^2/kg, the mortar fluidity was the best and had no apparent relationship with the PSD characteristics of GGBFS. With increasing the specific surface area of GGBFS, the mortar fluidity gradually

TABLE 2 The particle characteristics of GGBFS.

Sample	Characteristic particle size D_e (μm)	Uniformity coefficient n	Correlation coefficient R	Blaine specific surface area (m^2/kg)
S1	8.0	0.94	0.994	1,003
S2	8.0	1.00	0.995	1,001
S3	8.0	1.11	0.993	873
S4	8.0	1.20	0.997	772
S5	8.1	1.30	0.993	602
S6	8.0	1.40	0.992	469
S7	12.0	0.90	0.992	851
S8	12.0	1.00	0.994	732
S9	12.1	1.10	0.996	551
S10	12.0	1.20	0.999	402
S11	12.0	1.30	0.998	370
S12	12.0	1.37	0.994	350
S13	16.0	0.90	0.993	588
S14	16.0	1.00	0.997	492
S15	16.0	1.10	0.997	368
S16	16.1	1.20	0.996	343
S17	16.0	1.29	0.995	291
S18	20.1	0.90	0.995	474
S19	20.1	1.00	0.997	322
S20	20.1	1.06	0.998	321
S21	20.1	1.11	0.999	289
S22	20.0	1.15	0.999	286

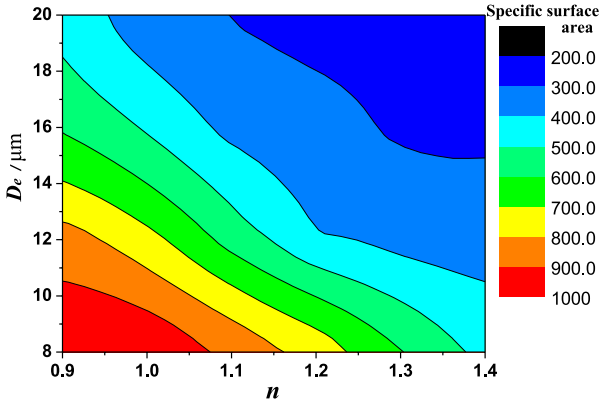

FIGURE 1
The relationships between the specific surface area, D_e and n.

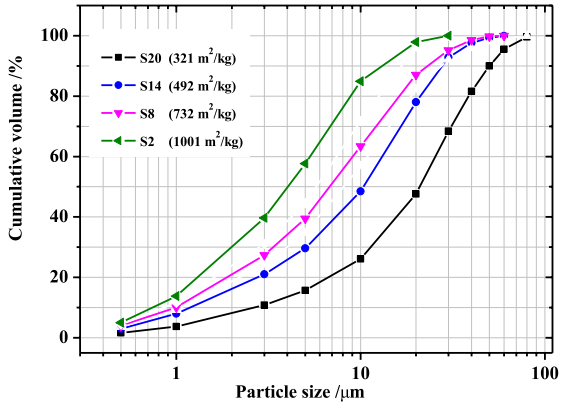

FIGURE 2
The particle size distribution of GGBFS.

decreased. From Figure 5, the specific surface area of GGBFS powder and mortar compressive strength at 7 days had an approximately linear relationship. Figure 6 shows that the relationship between the mortar strength at 28 days and the PSD substantially changed. When D_e = 8 μm and n = 1.4, the mortar compressive strength at 28 days was the highest.

Mortar fluidity and strength of GGBFS with PCE

PCE was added at a concentration of 0.6% during mortar molding, producing a dispersion effect. The resulting influence of the PSD characteristics (D_e and n values) of each test GGBFS

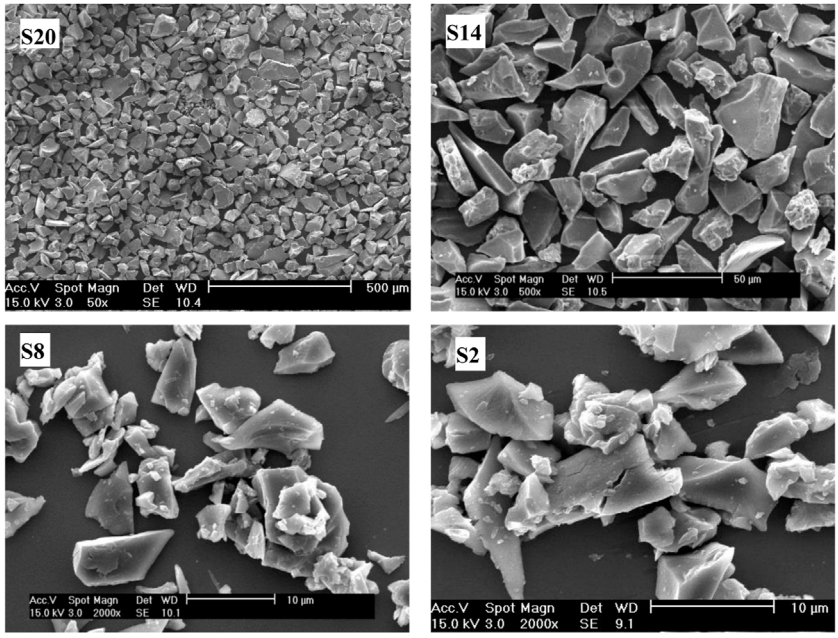

FIGURE 3
The particle morphologies of GGBFS.

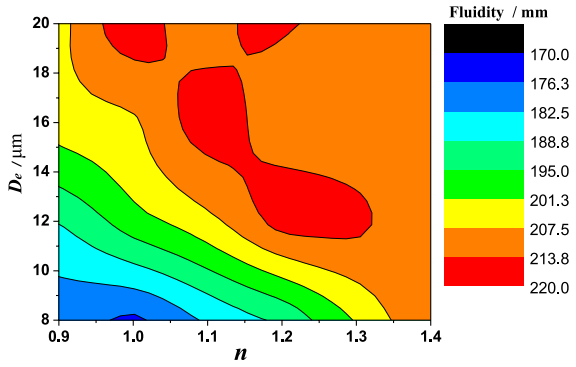

FIGURE 4
The influence of the PSD characteristics on mortar fluidity without PCE.

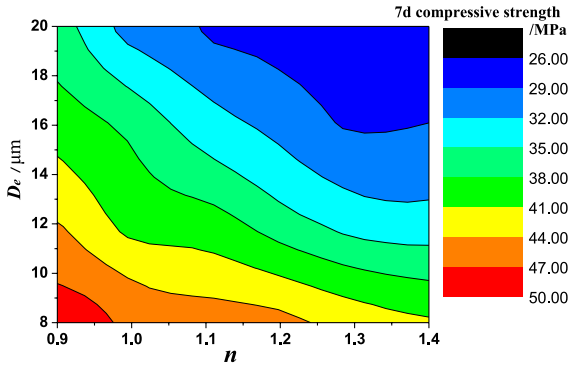

FIGURE 5
The influence of the PSD characteristics on 7-day mortar compressive strength without PCE.

powder on mortar fluidity and activity indexes, as well as their trends, are shown in Figures 7–9.

From Figure 7, with the addition of PCE, the larger the specific surface area of GGBFS powder was, the higher the mortar fluidity. Given the same specific surface area of GGBFS powder, when the PSD was located on the diagonal line between the left bottom corner and right upper corner in Figure 7, the mortar fluidity was relatively low, indicating that mortar fluidity was related to the PSD characteristics of the GGBFS powder.

According to Figures 8, 9, the relationship between the mortar strength and PSD of GGBFS with the addition of PCE was remarkably different from that without PCE. The overall trend showed that the higher the specific surface area of GGBFS powder was, the larger the compressive strength of mortar paste at 7 days. However, with an increase in the D_e of the GGBFS powder, the enhancement in the mortar compressive strength at 7 days due to the increase in the specific surface area of the GGBFS powder gradually declined, and an increase in the specific

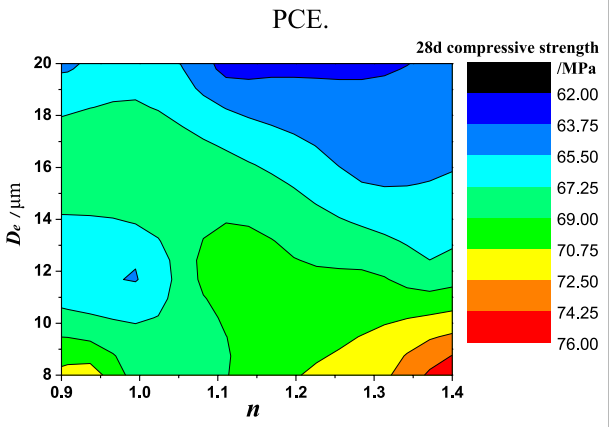

FIGURE 6
The influence of the PSD characteristics on 28-day mortar compressive strength without PCE.

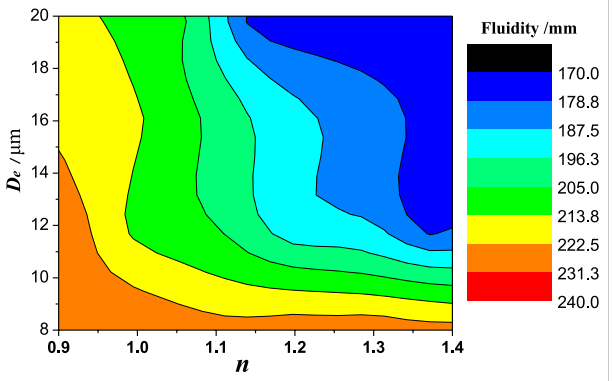

FIGURE 7
The influence of the PSD characteristics on mortar fluidity with PCE.

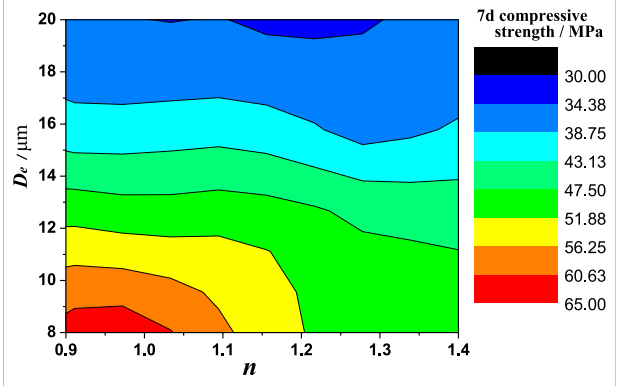

FIGURE 8
The influence of the PSD characteristics on 7-day mortar compressive strength with PCE.

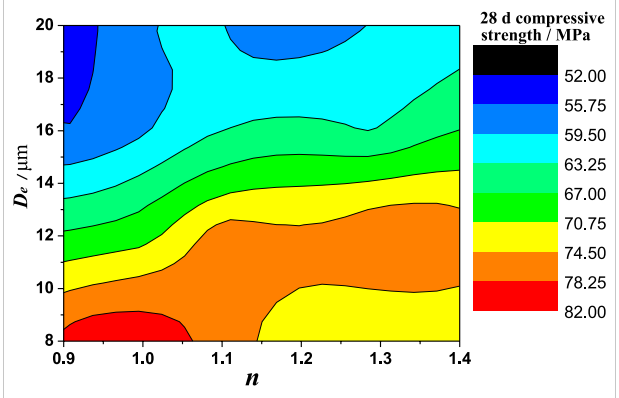

FIGURE 9
The influence of the PSD characteristics on 28-day mortar compressive strength with PCE.

surface area was caused by a decrease in n. When the mortar was cured for 28 days, the above phenomena became more obvious. Thus, when the D_e of the GGBFS powder was more than 10 μm, n increased, the specific surface area decreased, and the mortar strength increased.

Analysis and discussion

Influence of particle size distribution of GGBFS powder on mortar fluidity

The PSD characteristics of GGBFS powder had an impact on the mortar fluidity and strength. Interparticle forces between GGBFS powders, especially microfine GGBFS powders, are an important factor influencing cement-GGBFS mortar fluidity. When the fineness of GGBFS powder is too high, aggregation will occur between microfine particles of GGBFS. The resulting aggregates could absorb more moisture, reducing the lubrication effect of free water on friction between moving material objects, which could lead to a reduction in mortar fluidity. When the fineness of GGBFS powder is too low, the tendency of mortar segregation and bleeding will increase, which would also lead to a reduction in mortar fluidity. Among the four groups of GGBFS powders without PCE and with different D_e values, when the mortar fluidity was the best, the contents of particles with sizes of 5–10 μm and 10–15 μm were relatively high in each group of GGBFS powders. In particular, the mass fraction of 10–15 μm size particles in GGBFS powder was highly related to mortar fluidity. This relationship indicated that GGBFS powders with a size of 10–15 μm had an insignificant aggregation tendency and

relatively small sedimentation rate, which thus improved mortar fluidity.

After the addition of PCE, the GGBFS powders could disaggregate. When the specific surface area of GGBFS powder was larger, the secondary filling of GGBFS powder between cement particles was enhanced, thus also improving mortar fluidity. The reason is that the PCE added in this study was prepared by polymerization of acrylic acid, using α-methallyl-ω-hydroxy poly ethylene glycol (HPEG) as a macromonomer. This is a kind of PCE with a comb-branched chain molecular structure. PCE is dispersed by adsorption on the surface of GGBFS powders. The adsorption is realized by the anion anchoring group (such as carboxylic acid group) on the main chain of PCE molecule. The long branch chain of PCE is composed of polyoxyethylene (PEO), which is a non-ionic strong polar group. One end of the branch chain is connected with the hydrophobic main chain through ether bond, and the other end is connected with PEO with strong hydrophilicity. This molecular structure can fully extend the long branched chain in the aqueous solution to form a thick solvated outer layer, resulting in steric hindrance, which significantly enhances the dispersion of PCE.

Influence of particle size distribution of GGBFS powder on mortar strength

When there was no addition of PCE, the strength of cement-GGBFS mortar at 7 days exhibited a linearly increasing relationship with the specific surface area of GGBFS powder. This relationship occurred because when GGBFS powder fineness increases, the hydration activity is enhanced, and therefore the mortar strength also increases. When cured for 28 days, the density of the hardened mortar was significantly increased, and aggregation of GGBFS powder became the major factor limiting increases in strength. This limiting effect occurs because when rapid hydration and hydration product layer formation occur on the outer surface of GGBFS aggregates in the early stage of hydration, the migration and diffusion of Ca^{2+}, OH^{-}, and H_2O to the inner layer are inhibited, which hinders the hydration of the GGBFS particles inside the aggregates, prevents effective entanglement between particles, and is not conducive to the development of material strength. The higher the content of microparticles in GGBFS powder is, the stronger this effect. Therefore, in order to improve the activity indexes of GGBFS, the overall fineness of the powder should be improved, and the proportion of microparticles in the powder should be controlled. GGBFS powders conforming to these requirements must have a high specific surface area and narrow PSD.

When PCE was added during the cement-GGBFS mortar preparation process and the water-mortar ratio was appropriately reduced, the structure and hydration process of the mortar changed greatly as follows: 1) due to the dispersion effect of PCE, the number and size of aggregates of GGBFS powder were greatly reduced, strengthening the correlation between the microaggregate effect of the GGBFS powder and the material strength from the material structure; 2) the dispersion effect of PCE reduced the average distance between particles and enhanced the initial density of the hardened mortar.

After adding PCE, the effect of GGBFS powder aggregation on mortar strength weakened, and the influence of the dense-packing effect caused by the PSD of the cement material on mortar strength was enhanced. The PSD of the cement used in the experiment (D_e = 25.5 μm, n = 1.10) is in the upper left corner of Figures 7–9. When the D_e of the GGBFS powder was maintained and n was increased, the distance between the points corresponding to the PSD of the GGBFS powder (D_e, n) and that of the cement increased, and the mortar strength developed steadily. If the n of the GGBFS powder was fixed at 0.9, the closer the points corresponding to the PSD of the GGBFS powder and that of the cement were to one another, the lower the mortar strength. When the overall particle size of the GGBFS powder was significantly smaller than that of the Portland cement and its PSD was narrow, the combination of the two components benefited the secondary filling of GGBFS powder between cement particles, and the aggregation effect of the fine powder was low, thus resulting in a greater strengthening effect in the hardened mortar. It can be seen that in the grinding process of GGBFS, by adjusting the operation parameters of the high-efficiency separator, appropriately reducing the D_e and increasing n of the GGBFS powder can be achieved, which can reduce the power consumption of grinding and improve the quality of the GGBFS powder while keeping the specific surface area of the GGBFS powder unchanged. This finding has great engineering application value.

Chemically bound water of the hardened pastes

Four test GGBFS powders with similar specific surface areas were mixed with cement to prepare cement-GGBFS paste. After curing at different ages, the determination results of chemically combined water of cement-GGBFS pastes are shown in Figure 10.

It can be seen from Figure 10 that at the early stage of hydration, the chemically combined water of the hardened cement-GGBFS paste is lower than that of the cement paste. This is because the early hydration activity of GGBFS is low and the hydration rate is very slow, so the early chemically combined water mainly comes from the hydration products of cement. With the increase of hydration time, the chemical bond water of cement-GGBFS paste is higher than that of cement paste. After 28 days of curing, the chemical bond water of cement-GGBFS paste is up to 13% higher than that of cement paste. This fully shows that the late hydration rate of GGBFS is higher than that of

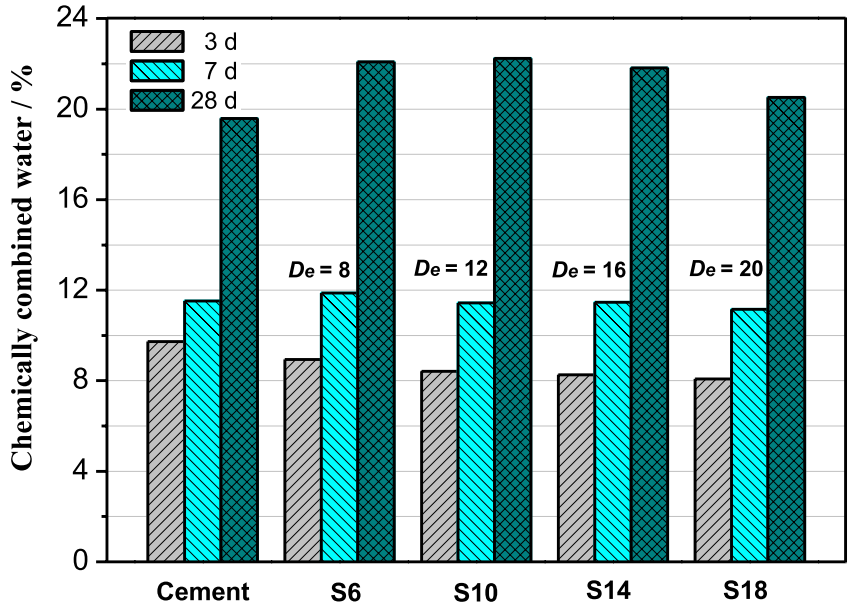

FIGURE 10
Chemically combined water of cement-GGBFS pastes.

Portland cement when it is used in combination with cement, which also provides an important basis for the experimental result that the hydration activity index of GGBFS in the above experiment is generally higher than 1.0.

Under the same curing age, the chemically combined water of cement-GGBFS paste decreases with the increase of the characteristic particle size and uniformity coefficient of cement-GGBFS paste. This is because with the extension of curing age, cement hydration generates a large amount of $Ca(OH)_2$, which fully stimulates the activity of GGBFS. The pozzolanic reaction of GGBFS generates C-S-H gel, which increases the chemically combined water of hardened composite paste. In addition, the hydration reaction of GGBFS needs to consume $Ca(OH)_2$, which will further promote the hydration of cement and generate more hydration products.

Interfacial structure of hydration products

Figure 11 shows SEM images of the interfacial structure and hydration products of three cement-GGBFS pastes. From the SEM images of 7-day cement-GGBFS hardened pastes, it can be seen that the overall hydration degree of the composite cementitious materials is not high, and there are a large number of unhydrated GGBFS particles. For large GGBFS particles with a particle size of more than 10 μm, only a small amount of hydration occurs on the surface of the particles, and the resulting hydration product cannot cover the entire particle. Small particles with a particle size below 1 μm have a higher degree of hydration, and most of the surface is completely wrapped by hydration products. The smaller the particle size of GGBFS particles is, the higher the degree of hydration will be. Due to the low degree of hydration, only a small amount of hydration products are bonded between the particles, and there are a large number of voids to be filled, so the 7-day hydration hardened paste of cement-GGBFS is difficult to compact.

The pastes that had been cured for 28 days have a much denser interfacial structure and contain a significantly larger number of dendritic C-S-H hydration products distributed in clusters, which formed a relatively widely connected network. The hydration products are flocculent colloids and are compact in structure, wrapped with small particles, and attached to the surface of large particles. With the decrease of particle size of GGBFS particles, no hexagonal $Ca(OH)_2$ euhedral crystals were observed in this paste. This indicates that the composite cementitious materials had a high capacity to absorb $Ca(OH)_2$ in the cement paste and became hydrated relatively quickly during the later stage of curing.

The typical hydration product region was selected and the composition of hydration product was analyzed by EDS. EDS analysis results show that the main elements of hydration products are Ca, Si, and O, and also contain certain Al and Mg. This is because blast furnace slag contains more Al and Mg,

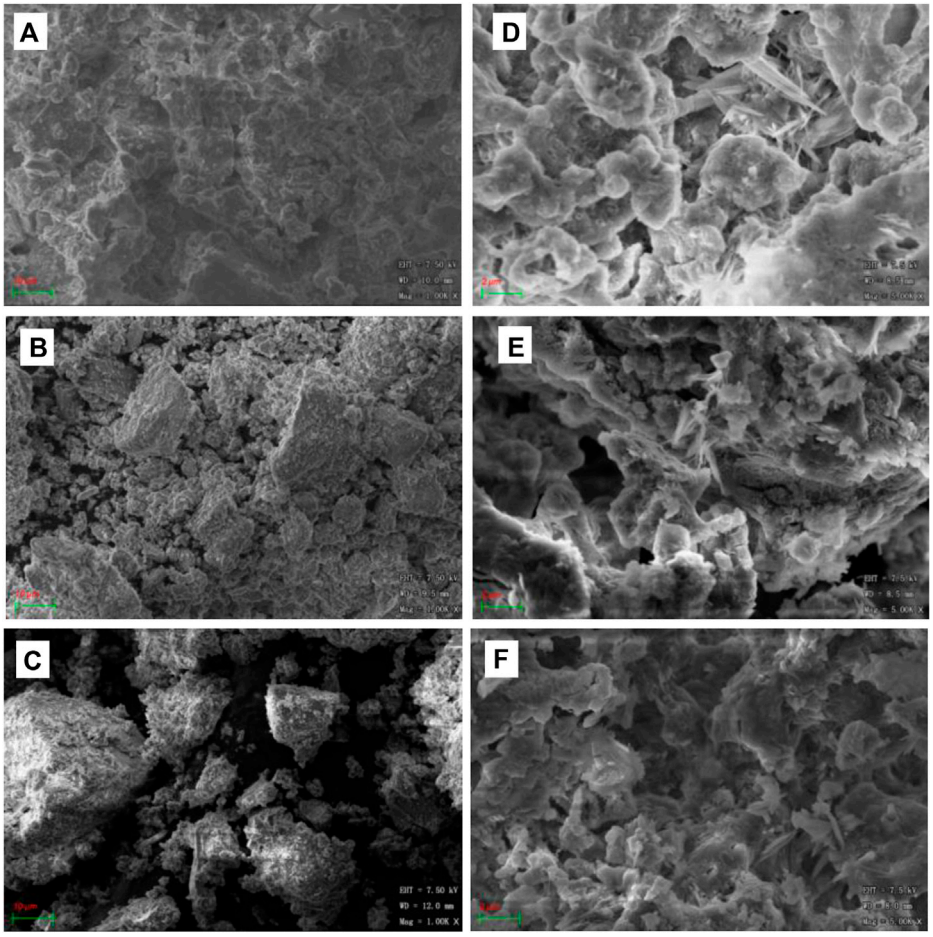

FIGURE 11
SEM images of morphologies of cement-GGBFS hydration products. **(A–C)**: S2, S4, and S6 at 7 days; **(D–F)**: S2, S4, and S6 at 28 day.

which can form a certain C-A-S-H gel. The Ca/Si molar ratio at each EDS site was calculated and the average value was calculated. The Ca/Si ratio of the hydration product is between 1.26 and 1.42, and the average value is 1.38. The Ca/Si ratio of C-S-H gel generated by cement hydration is usually between 1.5 and 2.0, or higher (Richardson, 1999). In the cement-GGBFS composite cementitious system, the Ca/Si ratio of the generated C-S-H gel was lower than that of the cement. With the decrease of GGBFS particle size, the Ca/Si of C-S-H gel decreases, which is due to the relatively low Ca/Si in the gel generated by GGBFS hydration.

Conclusions

When PCE is not added, the aggregation of GGBFS has a great negative effect on the mortar fluidity and hardened paste strength. With decreasing the characteristic particle size D_e and uniformity coefficient n of GGBFS powder, the mortar fluidity decreased rapidly. After adding PCE, the influence of the D_e of the GGBFS powder on mortar strength was greater than that of n on mortar strength. When the specific surface area of GGBFS is the same, greater strength of hardened paste can be obtained by simultaneously reducing the D_e and improving the n of the GGBFS powder.

Data availability statement

The original contributions presented in the study are included in the article/Supplementary Material; further inquiries can be directed to the corresponding author.

Author contributions

ZL: Writing—Original Draft, Conceptualization, Methodology; TH: Writing—Review and Editing, Funding

acquisition; ZX:Data Curation; XZ:Resources, Supervision; SZ: Project administration ;YL: Resources.

Funding

This study and the completion of this paper were supported by the Guangdong Basic and Applied Basic Research Foundation (2022A1515010508, 2021A1515010671, and 2020A1515011221); Innovation and Entrepreneurship Training Program for College Students of Guangdong Province (S202210576053); and the Key construction discipline scientific research capability improvement project of Guangdong Province (2021ZDJS071).

Conflict of interest

The authors declare that the research was conducted in the absence of any commercial or financial relationships that could be construed as a potential conflict of interest.

Publisher's note

References

Abu-Eishah, S. I., El-Dieb, A. S., and Bedir, M. S. (2012). Performance of concrete mixtures made with electricarcfurnace (EAF) steel slag aggregate produced in the Arabian Gulf region. *Constr. Build. Mat.* 34, 249–256. doi:10.1016/j.conbuildmat.2012.02.012

Akca, A. H., and Zihnioğlu, N. Ö. (2013). High performance concrete under elevated temperatures. *Constr. Build. Mat.* 44, 317–328. doi:10.1016/j.conbuildmat.2013.03.005

Binici, H., Aksogan, O., Cagatay, I. H., Tokyay, M., and Emsen, E. (2007). The effect of particle size distribution on the properties of blended cements incorporating GGBFS and natural pozzolan (NP). *Powder Technol.* 177, 140–147. doi:10.1016/j.powtec.2007.03.033

Camalan, M. (2019). Investigating the effects of random sieving losses on particle size distributions. *Part. Sci. Technol.* 39, 108–115. doi:10.1080/02726351.2019.1669749

Celik, I. B. (2009). The effects of particle size distribution and surface area upon cement strength development. *Powder Technol.* 188, 272–276. doi:10.1016/j.powtec.2008.05.007

Çetin, C., Erdoğan, S. T., and Tokyay, M. (2016). Effect of particle size and slag content on the early hydration of interground blended cements. *Cem. Concr. Compos.* 76, 39–49. doi:10.1016/j.cemconcomp.2015.12.001

Evi, A. S. (2017). A huge number of artificial waste material can be supplementary cementitious material (SCM) for concrete production—a review Part II. *J. Clean. Prod.* 142, 4178–4194. doi:10.1016/j.jclepro.2015.12.115

Gao, P., Zhang, T., Wei, J., and Yu, Q. J. (2018). Evaluation of RRSB distribution and lognormal distribution for describing the particle size distribution of graded cementitious materials. *Powder Technol.* 331, 137–145. doi:10.1016/j.powtec.2018.01.079

Horsfield, H. T. (1932). The strength of asphalt mixtures. *J. Soc. Chem. Ind.* 53, 107–115.

Isaia, G. C., Gastaldini, A. L. G., and Moraes, R. (2003). Physical and pozzolanic action of mineral additions on the mechanical strength of high-performance concrete. *Cem. Concr. Compos.* 25, 69–76. doi:10.1016/s0958-9465(01)00057-9

Juenger, M. C. G., and Siddique, R. (2015). Recent advances in understanding the role of supplementary cementitious materials in concrete. *Cem. Concr. Res.* 78, 71–80. doi:10.1016/j.cemconres.2015.03.018

Kashani, A., Nicolas, R. S., Qiao, G. G., Van Deventer, J. S. J., and Provis, J. L. (2014). Modelling the yield stress of ternary cement-slag-fly ash pastes based on particle size distribution. *Powder Technol.* 266, 203–209. doi:10.1016/j.powtec.2014.06.041

Kovtun, M., Kearsley, E. P., and Shekhovtsova, J. (2015). Chemical acceleration of a neutral granulated blast-furnace slag activated by sodium carbonate. *Cem. Concr. Res.* 72, 1–9. doi:10.1016/j.cemconres.2015.02.014

Kuhlmanm, K., Ellerbrock, H. G., and Sprung, S. (1985). Particle size distribution and properties of cement. Part I: strength of Portland cement. *Zem. Kalk. Gips* 6, 136–144.

Liu, J., Qin, Q., and Yu, Q. (2020). The effect of size distribution of slag particles obtained in dry granulation on blast furnace slag cement strength. *Powder Technol.* 362, 32–36. doi:10.1016/j.powtec.2019.11.115

Luo, T., Wang, Q., and Zhuang, S. Y. (2019). Effects of ultra-fine ground granulated blast-furnace slag on initial setting time, fluidity and rheological properties of cement pastes. *Powder Technol.* 345, 54–63. doi:10.1016/j.powtec.2018.12.094

Richardson, I. G. (1999). The nature of C-S-H in hardened cements. *Cem. Concr. Res.* 29, 1131–1147. doi:10.1016/s0008-8846(99)00168-4

Sprung, S., Kuhlmanm, K., and Ellerbrock, H. G. (1985). Particle size distribution and properties of cement Part II: water demand of Portland cement. *Zem. Kalk. Gips* 11, 275–281.

Teng, S., Lim, T. Y. D., and Divsholi, B. S. (2013). Durability and mechanical properties of high strength concrete incorporating ultra fine Ground Granulated Blast-furnace Slag. *Constr. Build. Mat.* 40, 875–881. doi:10.1016/j.conbuildmat.2012.11.052

Tsivilis, S., and Parissakis, G. (1995). A mathematical model for the prediction of cement strength. *Cem. Concr. Res.* 25, 9–14. doi:10.1016/0008-8846(94)00106-9

Tsivilis, S., Tsinmas, S., and Benetatou, A. (1990). Study on the contribution of the fineness on cement strength. *Zem. Kalk. Gips* 43, 26–29.

Wang, A., Zhang, C., and Zhang, N. (1999). The theoretic analysis of the influence of the particle size distribution of cement system on the property of cement. *Cem. Concr. Res.* 29, 1721–1726. doi:10.1016/s0008-8846(99)00148-9

Xiao, H., Liu, R., Zhang, F., Liu, M., and Li, H. (2018). Role of nano-SiO2 in improving the microstructure and impermeability of concrete with different aggregate gradations. *Constr. Build. Mat.* 188, 537–545. doi:10.1016/j.conbuildmat.2018.08.148

Ye, H., Gao, X., Wang, R., and Wang, H. (2017). Relationship among particle characteristic, water film thickness and flowability of fresh paste containing different mineral admixtures. *Constr. Build. Mat.* 153, 193–201. doi:10.1016/j.conbuildmat.2017.07.093

Yu, R., Spiesz, P., and Brouwers, H. J. H. (2015). Development of an eco-friendly Ultra-High Performance Concrete (UHPC) with efficient cement and mineral admixtures uses. *Cem. Concr. Compos.* 55, 383–394. doi:10.1016/j.cemconcomp.2014.09.024

Zhang, G., and Li, G. (2016). Effects of mineral admixtures and additional gypsum on the expansion performance of sulphoaluminate expansive agent at simulation of mass concrete environment. *Constr. Build. Mat.* 113, 970–978. doi:10.1016/j.conbuildmat.2016.03.131

Zhao, J., Wang, D., and Yan, P. (2017). Design and experimental study of a ternary blended cement containing high volume steel slag and blast-furnace slag based on Fuller distribution model. *Constr. Build. Mat.* 140, 248–256. doi:10.1016/j.conbuildmat.2017.02.119